0026-895X/90/040517-07$03.00/0

MOLECULAR PHARMACOLOGY, 38:517-523

Delineation of Muscarinic Receptor Domains Conferring Selectivity of Coupling to Guanine Nucleotide-Binding Proteins and Second Messengers

JÜRGEN WESS, TOM I. BONNER, FRANK DÖRJE, and MARK R. BRANN

Laboratory of Molecular Biology, National Institute of Neurological Disorders and Stroke (J.W., F.D., M.R.B.), and Laboratory of Cell Biology, National Institute of Mental Health (T.I.B.), National Institutes of Health, Bethesda, Maryland 20892

Received March 23, 1990; Accepted July 2, 1990

SUMMARY

The cloning and functional expression of five mammalian muscarinic acetylcholine receptor genes (m1–m5) has revealed that m1, m3, and m5 primarily couple to stimulation of phosphoinositide (PI) turnover, whereas m2 and m4 are strongly linked to inhibition of adenylate cyclase, albeit not exclusively. To identify the structural domains responsible for this functional specificity, cDNAs encoding chimeric m2/m3 receptors were constructed. The abilities of these receptors to mediate stimulation of PI hydrolysis and inhibition of prostaglandin E_2-stimulated cAMP accumulation, as well as the pertussis toxin (PTX) sensitivity of these responses, were examined after stable expression in mouse A9 L cells. Substitution of the putative third cytoplasmic loop (i3) of m2 with the corresponding m3 sequence resulted in a chimeric receptor that, similar to m3, stimulated PI breakdown by a PTX-insensitive mechanism but did not inhibit adenylate cyclase. Conversely, a chimeric m3 receptor containing the i3 domain of m2 showed the same functional profile as m2 (i.e., inhibition of adenylate cyclase and weak stimulation of PI turnover by a PTX-sensitive mechanism), indicating that the i3 loop is sufficient to determine coupling selectivity. Similarly, exchange of a short N-terminal segment of i3 (16 or 17 amino acids) between m2 and m3 resulted in chimeric receptors that gained the ability to mediate the functional responses of the wild-type receptor from which the segment was derived, although with substantially reduced efficiency. However, the chimeric m2 receptor containing the 17-amino acid m3 sequence in the N-terminal portion of i3 retained its ability to inhibit adenylate cyclase. Carbachol binding studies involving the use of the GTP analog 5′-guanylyl imidodiphosphate and PTX-pretreated cells generally correlated well with the functional findings. Our data indicate that the N-terminal portion of i3 is a sufficient but not the exclusive determinant of coupling selectivity displayed by the various muscarinic receptors.

Muscarinic receptors are coupled via G proteins to a variety of second messengers and ion channels (1). The cloning of five muscarinic receptor genes (m1–m5) from various mammalian species (2–9) has revealed that the muscarinic receptor family exhibits substantial structural homology with all G protein-coupled neurotransmitter receptors that have been cloned so far. Hydrophobicity analysis of the deduced amino acid sequences predicts that all of these receptors have similar structures, composed of seven hydrophobic membrane-spanning domains connected by alternating cytoplasmic and extracellular loops (10).

The functional expression of the different muscarinic receptor genes in mammalian cells and *Xenopus* oocytes has shown that the individual receptor subtypes preferentially couple to distinct signal transduction pathways (11–20). m1, m3, and m5 mediate a pronounced stimulation of PI hydrolysis (7–9, 13, 16, 17), an increase in intracellular calcium (15, 18), arachidonic acid release (13), and cAMP levels (17, 19), and the activation of calcium-dependent ion channels (11, 12, 15, 16, 18, 20). Usually, these effects are not (8, 16, 18, 19) or are only partially (21) sensitive to blockade by PTX. In contrast, m2 and m4 are linked to inhibition of adenylate cyclase (17, 19) and a weak stimulation of PI breakdown (17) via PTX-sensitive G proteins (19, 21, 22).

A recent electrophysiological study has found that the putative third cytoplasmic loop (i3) located between the fifth and the sixth transmembrane regions is sufficient to determine the specificity of the functional response mediated by the individual muscarinic receptors (23). This conclusion is based on the observation that exchanging the i3 domain between m1 and m2 caused a reversal in the ability of the resulting hybrid receptors

J.W. and F.D. were supported by grants from the Deutsche Forschungsgemeinschaft and the Stiftung Stipendien-Fonds des Verbandes der Chemischen Industrie, respectively.

ABBREVIATIONS: G protein, guanine nucleotide-binding protein; NMS, *N*-methylscopolamine; PTX, pertussis toxin; Gpp(NH)p, 5′-guanylyl imidodiphosphate; PI, phosphoinositide; IP_1, inositol monophosphate; i3, the putative third cytoplasmic loop of guanine nucleotide-binding protein-coupled receptors; PGE_2, prostaglandin E_2; HEPES, 4-(2-hydroxyethyl)-1-piperazineethanesulfonic acid; IBMX, 3-isobutyl-1-methylxanthine.

to couple to specific ion channels when expressed in *Xenopus* oocytes (23).

Except for the first and the last 15–20 amino acids, there is no apparent sequence homology in the i3 regions of m1–m5. Whereas the C-terminal sequences of i3 are relatively well conserved among all five receptors, the N-terminal portions are highly conserved only within the two functional classes (m1, m3, and m5 versus m2 and m4) (2–9). In agreement with this pattern, there exists considerable sequence similarity in the N-terminus of i3 between a cloned *Drosophila* muscarinic receptor that strongly couples to stimulation of PI metabolism and m1, m3, and m5 (24). On the other hand, a cloned chick muscarinic receptor that preferentially couples to inhibition of adenylate cyclase shares a high degree of sequence homology with m2 and m4 in this receptor domain (25).

To study the potential role of the N-terminal portion of i3 in conferring coupling selectivity, we have constructed cDNAs encoding chimeric m2/m3 receptors in which the whole i3 loop or a 16- or 17-amino acid segment located at the N-terminus of i3 has been exchanged between the human m2 and the rat m3 receptor (Fig. 1). Following stable expression of these receptors in mouse A9 L cells, their ability to mediate agonist-induced stimulation of PI hydrolysis and inhibition of PGE_2-stimulated adenylate cyclase activity has been investigated. In addition, the sensitivity of these responses to blockade by PTX has been examined, to allow a better characterization of the G proteins involved. Moreover, we have studied the agonist-binding properties of the various receptors involving the use of the GTP analog Gpp(NH)p and PTX-pretreated cells. Our data indicate that the N-terminal portion of i3 is a major but not the exclusive determinant of G protein coupling selectivity.

Experimental Procedures

Materials. Tissue culture reagents were from GIBCO Laboratories. [^{3}H]NMS (71–85 Ci/mmol) was purchased from New England Nuclear, and *myo*-[^{3}H]inositol (23 Ci/mmol) from American Radiolabeled Chemicals Inc. PTX and Gpp(NH)p were from List and Boehringer Mannheim, respectively. A9 L cells were obtained from the American Type Culture Collection and are a fibroblast-like subclone of the mouse cell line ATCC CCL 1. Reagents for the determination of cAMP by radioimmunoassay were supplied by Dr. Gary Brooker (Georgetown University, Washington, DC). All other reagents were from Sigma, unless otherwise noted.

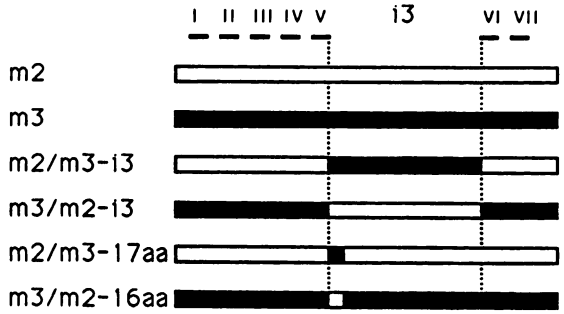

Fig. 1. Structure of chimeric muscarinic receptors composed of human m2 (□) and rat m3 sequences (■). The seven putative transmembrane domains are numbered I–VII from the NH_2-terminus (extracellular) to the COOH-terminus (intracellular). The putative third cytoplasmic loop is designated i3. The fact that m3 differs from m2 in the lengths of the N-terminal portion preceding transmembrane segment I (+44 amino acids), the i3 domain (+59 amino acids), and the C-terminal sequence following segment VII (+20 amino acids) is ignored. In total, the human m2 and the rat m3 receptors are composed of 466 and 589 amino acids, respectively (6). The individual chimeric receptors are composed as follows (amino acid numbers are given in parentheses): m2/m3-i3, m2 (1–207), m3 (252–491), and m2 (389–466); m3/m2-i3, m3 (1–251), m2 (208–388), and m3 (492–589); m2/m3-17aa, m2 (1–207), m3 (252–268), and m2 (225–466); m3/m2-16aa, m3 (1–251), m2 (208–223), and m3 (268–589).

Expression plasmid constructs. The construction of the expression plasmids coding for the human m2, the rat m3, and the various chimeric receptors examined in this study has been described previously (6, 26). To create mutant receptors m2/m3-i3 and m3/m2-i3, amino acids 208–388 from human m2 and amino acids 252–491 from rat m3 (i.e., the whole i3 domains) were exchanged (for sequences, see Ref. 7). Chimeric receptors m2/m3-17aa and m3/m2-16aa were constructed by substituting the amino acid sequences HISRASKSRIKKDKKE (m2) and RIYKETEKRTKELAGLQ (m3) located in the N-terminal portion of i3 for the corresponding 16 or 17 amino acids of m2 and m3. To create m2/m3-17aa, a *Hpa*I site was introduced at amino acids 225–226 in the i3 region of m2, changing amino acid 226 from alanine to asparagine (26).

Tissue culture and stable expression of cloned receptors. A9 cells were grown as monolayers in Dulbecco's modified Eagle's medium supplemented with 10% fetal calf serum and 100 units/ml penicillin and streptomycin, in 5% CO_2 at 37°. For transfections, cells were seeded into six-well plates at a density of 10^5 cells/well; 24 hr later, 4 μg of plasmid DNA [containing the muscarinic constructs inserted into the pCD expression vector, (27)] were cotransfected with 0.2 μg of pCDneo into A9 L cells by calcium phosphate precipitation, according to the procedure described by Chen and Okayama (28). Selection with the neomycin analog G418 (400 μg/ml) was started 72 hr after transfection and continued for 2–3 weeks. Clonal cell lines were obtained by single-cell cloning and assayed for [^{3}H]NMS binding capacity as described previously (29).

Binding assays. Cell membranes were obtained and binding assays were performed essentially as described previously (29). Binding buffer consisted of 25 mM sodium phosphate (pH 7.4) containing 5 mM $MgCl_2$. In order to determine [^{3}H]NMS affinities and maximum binding capacities for the various receptors and cell lines studied, six or seven different concentrations of the radioligand, ranging from 12.5 to 800 pM, were used. In the carbachol displacement experiments, 10–13 different carbachol concentrations, ranging from 0.63 nM to 3 mM, were employed. The [^{3}H]NMS concentration used in these experiments was 200 pM. Nonspecific binding was defined by 1 μM atropine. Incubations were carried out at room temperature for 3 hr. Binding data were analyzed by a nonlinear least squares curve-fitting procedure, as detailed in Ref. 29, using the program DATAPLOT run on a VAX II computer.

Protein concentrations were determined according to the method of Bradford (30), using a Bio-Rad protein assay kit.

PI metabolism. A9 L cells were incubated in 24-well plates (plating density, 10^5 cells/well) with 1 μCi/ml *myo*-[^{3}H]inositol for 48 hr. Immediately before an experiment, the cells were washed twice with phosphate-buffered saline and incubated for 15 min in Eagle's medium containing 10 mM LiCl and 20 mM HEPES. The medium was then replaced by 0.25 ml of the same medium containing the experimental agents. After a 1-hr incubation at room temperature, the reaction was stopped by the addition of 0.75 ml of 7.5% (w/v) ice-cold trichloroacetic acid, followed by a 30-min incubation on ice. The trichloroacetic acid was extracted with water-saturated diethyl ether (3 × 4 ml), and levels of IP_1 were determined by anion exchange chromatography (31) and an LKB liquid scintillation counter.

Measurement of cAMP levels. A9 L cells were plated at a density of 10^5 cells/well in 24-well plates. After 24 hr, the growth medium was replaced with 0.25 ml of Eagle's medium containing 1 mM IBMX, 20 mM HEPES, and the various carbachol concentrations to be tested. The reaction was stopped after a 10-min incubation at room temperature by addition of 0.25 ml of an ice-cold solution containing 0.1 N HCl

and 1 mM $CaCl_2$. cAMP levels were determined using a GAMMAFLOW automated radioimmunoassay for acetylated cAMP (^{125}I-acetyl-cAMP).

Results

[^{3}H]NMS binding studies. Transfected A9 L cells were examined for their ability to specifically bind the muscarinic antagonist [^{3}H]NMS. Whereas no detectable binding was found in nontransfected cells, specific [^{3}H]NMS binding could be demonstrated in A9 L cell lines transfected with m2, m3, and the various mutant receptor genes. In Table 1, dissociation constants (K_D) for [^{3}H]NMS as well as levels of expression (fmol/mg of membrane protein) are given for the individual receptors. Whereas m2/m3-i3 and m2/m3-17aa bound the radioligand with affinities similar to that of m2 (K_D approximately 90 pM), m3, m3/m2-i3, and m3/m2-16aa displayed an approximately 2–3-fold higher [^{3}H]NMS affinity (K_D approximately 40 pM). Thus, the [^{3}H]NMS binding profile of m2 and m3 remained essentially unaltered by substitutions in the i3 region.

Carbachol binding experiments. The ability of the agonist carbachol to displace specific [^{3}H]NMS binding to the various wild-type and chimeric receptors was studied in the absence and presence of the hydrolytically stable GTP analog Gpp(NH)p (100 μM). In the absence of Gpp(NH)p, all carbachol inhibition curves were characterized by Hill coefficients substantially smaller than 1 (Table 2). In the presence of Gpp(NH)p, all curves were steepened and shifted to the right, consistent with each of the receptors being coupled to G proteins endogenous to A9 L cells (Fig. 2, Table 2). To further characterize the G proteins involved, the effect of pretreatment of transfected cells with PTX (100 ng/ml, 14 hr) on carbachol binding was also investigated. As illustrated in Fig. 2, PTX had no significant effect on carbachol binding to m3, m2/m3-i3, and m3/m2-16aa (Table 2). In the case of m2, m3/m2-i3, and m2/m3-17aa, PTX pretreatment led to a steepening and a rightward shift of the agonist binding curves. The PTX effects on carbachol binding were quantitatively similar to those of Gpp(NH)p in the case of m2 and m3/m2-i3 but did not reach the magnitude of the Gpp(NH)p shift in the case of m2/m3-17aa.

As observed previously (26), carbachol inhibited [^{3}H]NMS binding to m2 with substantially higher potency, compared with m3 (Table 2). This potency difference was reversed when the i3 loops were exchanged between the two wild-type receptors. In contrast, m2/m3-17aa and m3/m2-16aa showed IC_{50} values similar to those of m2 and m3, respectively (Table 2).

PI metabolism. The ability of m2, m3, and the chimeric m2/m3 receptors to mediate stimulation of PI hydrolysis was determined by studying carbachol-induced increases in intracellular IP_1 levels. Cells were incubated with carbachol for 60 min, because IP_1 levels were found to be maximally elevated after this period of time (data not shown). Untransfected A9 L cells did not exhibit any increase in IP_1 production above basal levels following addition of the agonist. Upon stimulation by carbachol, wild-type m3 mediated a strong increase in IP_1 production (maximum response, 572 ± 69%; Table 1), which was not inhibited by pretreatment of cells with PTX (14 hr, 100 ng/ml) (Fig. 3). In contrast, agonist stimulation of m2-expressing cells resulted in a moderate PI response (maximum IP_1 elevation, 61 ± 7%; Table 1), which proved to be highly sensitive to blockade by PTX (Fig. 3).

Likewise, all chimeric receptors studied, except m3/m2-16aa, reliably mediated carbachol-induced increases in IP_1 accumulation, albeit with considerably lower efficiency than wild-type m3 (Fig. 3, Table 1). Whereas PTX pretreatment had no inhibitory effect on the responses evoked by stimulation of m2/m3-i3 and m2/m3-17aa, it blocked IP_1 production induced by activation of m3/m2-i3 (Fig. 3). All carbachol effects on PI turnover could be completely antagonized by 10 μM atropine.

cAMP levels. The ability of m2, m3, and the various mutant receptors to mediate inhibition of PGE_2-stimulated cAMP accumulation was investigated. Transfected cells were incubated with carbachol for 10 min, after which time maximal cAMP responses were observed. PGE_2 treatment (100 μM) of A9 L cells resulted in a 6–8-fold increase in cAMP over basal levels. This response was inhibited by 42 ± 2% after stimulation of m2-expressing cells with carbachol (Fig. 4, Table 1). The carbachol EC_{50} for this effect (0.049 ± 0.005 μM) was approximately 50-fold lower than that obtained for m2-mediated stimulation of PI breakdown (2.5 ± 0.8 μM) (Table 1). Likewise, three of the four chimeric receptors studied, m3/m2-i3, m2/m3-17aa, and m3/m2-16aa, mediated a decrease in PGE_2-induced cAMP production, although with lower efficiency than m2 (Fig. 4, Table 1). These effects, as well as the m2-induced decrease in cAMP levels, were completely prevented by pretreatment with PTX (Table 3). In contrast, carbachol concen-

TABLE 1

Antagonist binding and functional profile of chimeric m2/m3 muscarinic receptors stably expressed in A9 L cells

In the [^{3}H]NMS binding studies, Hill coefficients were not significantly different from unity for any of the receptors studied. EC_{50} values for carbachol were determined graphically from plots of log carbachol concentration versus percentage response. Carbachol concentrations used ranged from 0.1 μM to 1 mM (PI assays) and from 1.52 nM to 3.33 μM (cAMP assays), respectively. Basal IP_1 levels as well as background and PGE_2-stimulated cAMP levels are given in the legends to Figs. 3 and 4, respectively. Data are presented as means ± standard errors of two or three (binding studies) or three to eight independent experiments (functional studies), each performed in duplicate.

Receptor	[^{3}H]NMS binding		Stimulation of IP_1 accumulation			Inhibition of PGE_2-stimulated cAMP production		
	K_D, [^{3}H]NMS	B_{max}	Maximum increase	PTX sensitivity	EC_{50}, carbachol	Maximum inhibition	PTX sensitivity	EC_{50}, carbachol
	pM	fmol/mg of protein	%		μM	%		μM
m2	91 ± 14	746 ± 2	61 ± 7	+	2.5 ± 0.8	42 ± 2	+	0.049 ± 0.005
m3	38 ± 1	618 ± 59	572 ± 69	−	4.4 ± 0.7	1 ± 1		
m2/m3-i3	88 ± 5	444 ± 16	73 ± 15	−	16.5 ± 4.2	1 ± 1		
m3/m2-i3	44 ± 5	113 ± 7	26 ± 5	+	ND[a]	18 ± 2	+	0.12 ± 0.01
m2/m3-17aa	95 ± 10	1023 ± 9	26 ± 2	−	20.4 ± 12.8	17 ± 1	+	0.22 ± 0.07
m3/m2-16aa	38 ± 3	471 ± 1	6 ± 4			11 ± 2	+	0.053 ± 0.018

[a] ND, not determinable with sufficient accuracy, due to the flatness of the dose-response curves.

TABLE 2

Parameters of carbachol binding to chimeric m2/m3 muscarinic receptors

Several different concentrations of the agonist carbachol (0.63 nM to 3 mM) were incubated at room temperature for 3 h with 200 pM [^{3}H]NMS. Membrane homogenates from transfected A9 L cells were assayed in the absence (control) or presence of Gpp(NH)p (100 μM). In addition, membrane homogenates from PTX-pretreated cells (100 ng/ml, 14 hr) were assayed in the absence of Gpp(NH)p. IC_{50} values and Hill coefficients (n_H) were obtained by computer fit, as described (29). Data are presented as means ± standard errors of three independent experiments, each performed in duplicate.

Receptor	Control		+Gpp(NH)p		+PTX	
	IC_{50}	n_H	IC_{50}	n_H	IC_{50}	n_H
	μM		μM		μM	
m2	0.064 ± 0.009	0.28 ± 0.02	4.28 ± 0.13	0.72 ± 0.02	3.20 ± 0.44	0.91 ± 0.05
m3	50.5 ± 0.9	0.70 ± 0.03	135 ± 10	0.97 ± 0.05	55.4 ± 3.7	0.69 ± 0.05
m2/m3-i3	17.8 ± 6.9	0.64 ± 0.17	57.2 ± 6.4	1.02 ± 0.07	18.6 ± 2.8	0.56 ± 0.05
m3/m2-i3	0.33 ± 0.04	0.53 ± 0.03	2.59 ± 0.05	0.62 ± 0.01	2.69 ± 0.26	0.62 ± 0.01
m2/m3-17aa	0.13 ± 0.04	0.48 ± 0.03	2.33 ± 0.51	0.80 ± 0.06	1.22 ± 0.24	0.62 ± 0.05
m3/m2-16aa	39.2 ± 1.7	0.59 ± 0.03	73.7 ± 5.2	0.83 ± 0.06	43.2 ± 4.6	0.56 ± 0.03

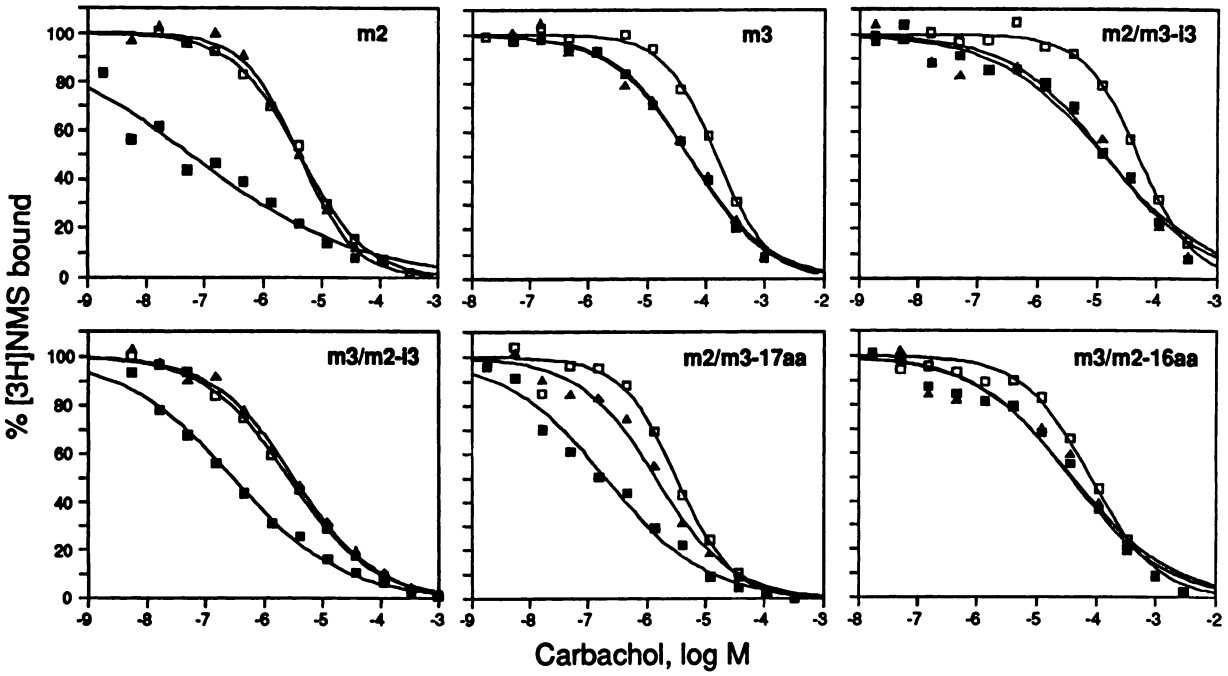

Fig. 2. Effect of Gpp(NH)p and PTX on carbachol binding to m2, m3, and chimeric m2/m3 receptors. The displacement of [^{3}H]NMS (200 pM) binding by carbachol was studied in membrane homogenates (10–40 μg of protein) from transfected A9 L cells. Assays were performed in the absence (control) (■) or presence of 100 μM Gpp(NH)p (□). In addition, membrane homogenates from PTX-pretreated cells (100 ng/ml; 14 hr) (▲) were assayed in the absence of Gpp(NH)p. *Lines* were generated by computer fit, as described (29). Curves shown are representative of three independent experiments, each performed in duplicate. Computer-fitted binding parameters are summarized in Table 2.

trations of up to 1 mM did not inhibit adenylate cyclase activity in cells expressing m3 and m2/m3-i3; instead, cAMP levels were slightly increased over PGE_2-stimulated levels (maximum increases, 38 ± 11 and 12 ± 8%, respectively; three experiments) at higher carbachol concentrations (3 μM to 1 mM). As shown with m1-expressing A9 L cells, this effect is most likely secondary to the carbachol-induced inositol phosphate release (32). All carbachol-induced changes in intracellular cAMP levels could be completely blocked by incubation with 10 μM atropine.

Discussion

To study the structural determinants underlying the functional diversity of muscarinic receptors, chimeric m2/m3 receptors were stably expressed in A9 L cells and examined for their ability to mediate stimulation of PI metabolism and inhibition of adenylate cyclase. All chimeric receptors studied bound the antagonist [^{3}H]NMS and the agonist carbachol in an affinity range comparable to that of the wild-type receptors. As has been observed in other cell lines (21, 22), we have shown that m2 receptors couple to two PTX-sensitive responses in A9 L cells, strong inhibition of adenylate cyclase and weak stimulation of PI metabolism. On the other hand, m3 receptors strongly stimulate PI turnover by a PTX-insensitive mechanism and do not inhibit adenylate cyclase.

When the i3 loops were exchanged between m2 and m3, the resulting chimeric receptors, m2/m3-i3 and m3/m2-i3, displayed the same functional profile as m3 and m2, respectively. These data confirm at a biochemical level that the i3 domain contains all of the information required to confer coupling selectivity, as observed in a recent electrophysiological analysis of m1/m2 receptor chimeras expressed in *Xenopus* oocytes (23). In that case, exchange of the i3 loops between m1 and m2 caused a reversal in the ability of the resulting mutant receptors to couple to calcium-dependent versus calcium-independent ion channels (23). Similar findings have been obtained with α_2/β_2 hybrid receptors (33), indicating that the i3 region may gener-

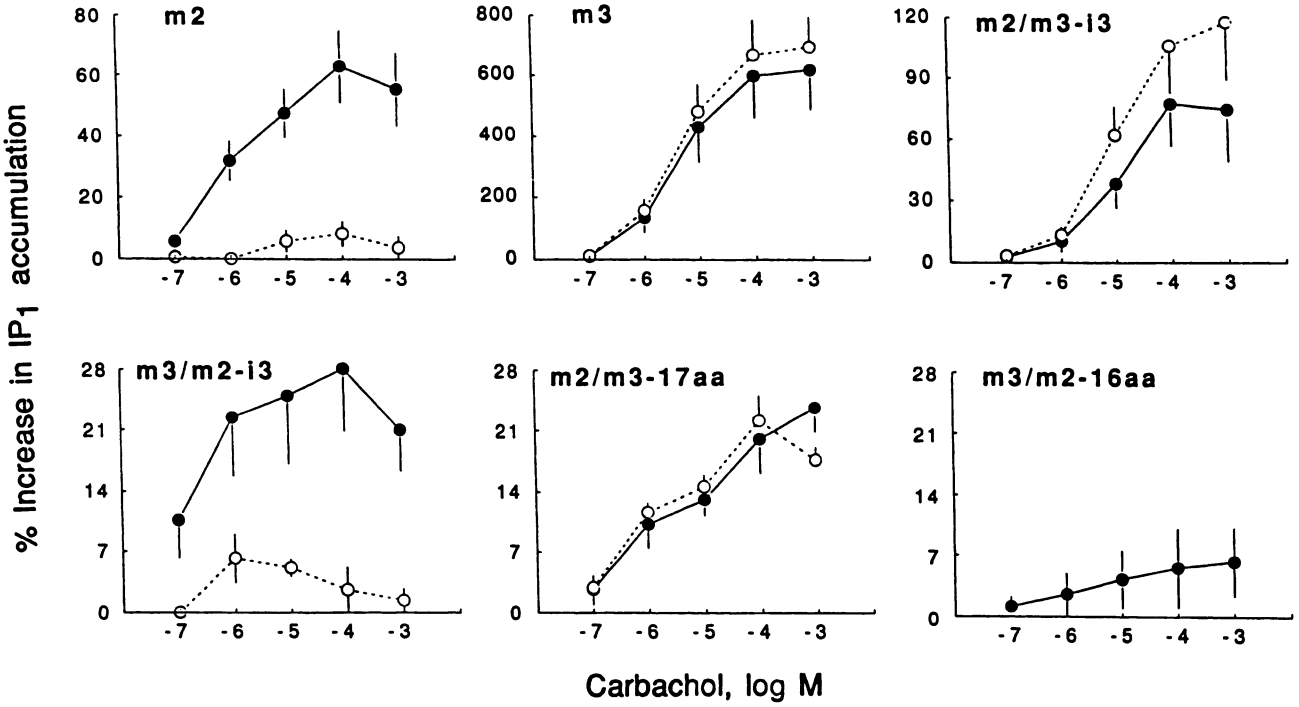

Fig. 3. Effect of PTX on receptor-mediated stimulation of PI hydrolysis. ●, Control responses (no pretreatment); ○, effects after incubation with PTX (100 ng/ml; 14 hr). A9 L cells expressing m2, m3, or the indicated chimeric receptors were incubated with increasing concentrations of carbachol for 60 min at room temperature, and the production of IP_1 was determined as described. The results are presented as percentage of increase in IP_1 above basal levels measured in the absence of carbachol. Basal IP_1 levels (in cpm/well) in nonpretreated cells were: 231 ± 9 (m2), 228 ± 23 (m3), 323 ± 15 (m2/m3-i3), 210 ± 18 (m3/m2-i3), 257 ± 20 (m2/m3-17aa), and 232 ± 21 (m3/m2-16aa). Basal IP_1 levels in PTX-pretreated cells were not significantly different from these values. No PTX experiments were carried out with m3/m2-16aa, because this mutant receptor did not mediate an appreciable PI response. Data are presented as means ± standard errors of three or four independent experiments, each performed in duplicate.

ally determine the effector coupling specificity of G protein-linked receptors.

It should be noted that the maximum functional responses mediated by m2/m3-i3 and m3/m2-i3 were weaker than the corresponding wild-type m2 and m3 effects, particularly as far as stimulation of PI hydrolysis is concerned. One possible explanation for this phenomenon is that other cytoplasmic domains, besides the i3 loop, which have little effect on coupling selectivity, may be required for full coupling efficiency. Alternatively, it is also conceivable that the chimeric receptors adopt a conformation that does not couple efficiently to the respective G proteins.

In order to more precisely define the portion(s) within the i3 domain responsible for the described functional selectivity, chimeric receptors (m2/m3-17aa and m3/m2-16aa) were constructed in which the N-terminal portion of i3 was exchanged between m2 and m3. It has been suggested that this receptor segment may play a critical role in selective receptor-G protein interactions (26), because it is conserved only within the two functional classes of muscarinic receptors (m1, m3, and m5 versus m2 and m4). In fact, the functional profiles of m2/m3-17aa and m3/m2-16aa clearly support this concept. Both mutant receptors gained the ability to mediate the functional responses of the respective wild-type receptor from which the short i3 fragment was derived, although with even lower efficiency than observed with m2/m3-i3 and m3/m2-i3. One possible explanation for the further reduction in activity is that additional domains within the i3 loop, besides the first 16 or 17 amino acids, are involved in defining the efficiency of coupling.

The presented data are in general agreement with our earlier study, which examined the ability of the same mutants to mediate stimulation of PI metabolism after transient expression in COS-7 cells (26). A notable difference between the results obtained in the two studies is that m2/m3-17aa was able to give a PI response in COS-7 cells similar in magnitude to that of wild-type m3, albeit with considerably reduced carbachol potency. The much higher levels of expression, on a per cell basis, that are achieved in the transient expression system may be an explanation for this discrepancy. When expressed at high levels, the weakly coupled chimeric receptor may behave in a fashion analogous to a partial agonist under conditions of a high degree of receptor spareness. Under such conditions, partial and full agonists display similar maximal responses.

Although our findings clearly demonstrate the pivotal functional role of the N-terminal section of i3, the activity profile of m2/m3-17aa indicates that this receptor domain is not the exclusive structural determinant of G protein coupling specificity. Despite the fact that m2/m3-17aa contains the m3 sequence in the N-terminal portion of i3, this receptor still couples to inhibition of adenylate cyclase, whereas m2/m3-i3, containing the whole i3 loop of m3, does not. This finding suggests that there exists an additional structural element within the i3 domain that is critically involved in conferring coupling selectivity. Biochemical analysis of m1 (34) and β_2 receptor (35) deletion mutants has shown that most of the i3 loop, except the two membrane-proximal portions, can be deleted without affecting coupling to stimulation of PI hydrolysis and cAMP production, respectively. It seems likely, therefore, that the C-terminal segment of i3, in addition to the N-terminus, contains

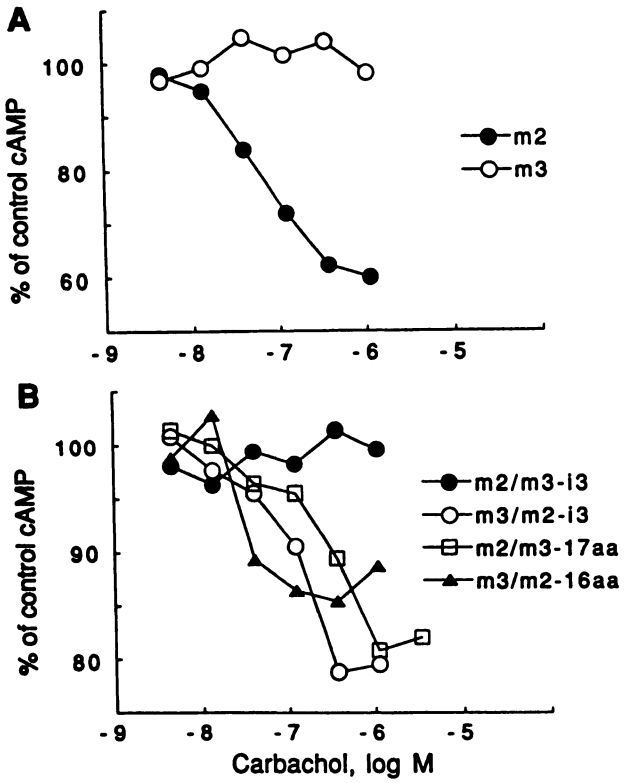

Fig. 4. Effect on PGE_2-induced cAMP accumulation mediated by m2 and m3 (A), as well as chimeric m2/m3 (B), receptors. Transfected A9 L cells were incubated for 10 min with increasing concentrations of carbachol, in the presence of PGE_2 (100 μM) and the phosphodiesterase inhibitor IBMX (1 mM). cAMP levels were determined by radioimmunoassay, as described. Before addition of PGE_2, cAMP levels in IBMX-treated cells were (in pmol/ml of assay medium; total assay volume/well, 0.5 ml): 2.10 ± 0.13 (m2), 1.82 ± 0.09 (m3), 2.64 ± 0.14 (m2/m3-i3), 2.34 ± 0.17 (m3/m2-i3), 2.05 ± 0.10 (m2/m3-17aa), and 2.06 ± 0.12 (m3/m2-16aa). PGE_2 increased these levels to 14.1 ± 2.0 (m2), 11.3 ± 1.2 (m3), 19.8 ± 3.8 (m2/m3-i3), 16.6 ± 2.0 (m3/m2-i3), 13.1 ± 2.2 (m2/m3-17aa), and 14.2 ± 1.2 (m3/m2-16aa). Data are expressed as percentage of control cAMP levels in the presence of PGE_2 and in the absence of carbachol. Data from a representative experiment are shown. Similar responses were obtained in three to six independent experiments, each performed in duplicate.

TABLE 3

Effect of PTX on carbachol-induced decreases in cAMP levels mediated by chimeric m2/m3 muscarinic receptors

Transfected A9 L cells were pretreated with PTX (100 ng/ml) for 14 hr. For cAMP assays, cells were incubated with 1.11 μM carbachol in the presence of PGE_2 (100 μM) and the phosphodiesterase inhibitor IBMX (1 mM). cAMP levels were measured by radioimmunoassay, as described in Experimental Procedures. Basal and PGE_2-stimulated cAMP levels were similar to the values given in the legend to Fig. 4. In PTX-pretreated cells, these levels were not significantly different from those found in nonpretreated cells. Data are expressed as percentage of control cAMP levels in the presence of PGE_2 and in the absence of carbachol. In the case of m3 and m2/m3-i3, no significant decrease in PGE_2-stimulated cAMP levels was observed, without or after pretreatment with PTX. Data are given as means ± standard errors of two independent experiments, each performed in duplicate.

	Inhibition of PGE_2-stimulated cAMP production	
	No pretreatment	+PTX
	%	
m2	41 ± 4	4 ± 3
m3/m2-i3	17 ± 2	2 ± 2
m2/m3-17aa	13 ± 3	3 ± 2
m3/m2-16aa	11 ± 2	2 ± 2

a second structural determinant of G protein coupling selectivity. Interestingly, m2/m3-17aa is also exceptional among all receptors studied in that it clearly couples to two different G proteins, a PTX-sensitive one mediating inhibition of adenylate cyclase and a PTX-insensitive one mediating stimulation of PI metabolism.

If coupling to PI turnover and inhibition of adenylate cyclase were governed by the same structural elements, one should expect that m3/m2-16aa, analogous to m2/m3-17aa, should retain its ability to induce stimulation of PI hydrolysis by a PTX-insensitive mechanism. However, no appreciable PI response was obtained with this mutant receptor. Given the relatively weak cAMP response mediated by m3/m2-16aa, a potential weak coupling of this receptor to PI hydrolysis may remain undetected due to the generally lower efficiency of coupling to PI turnover, as compared with the cAMP inhibition. In agreement with this concept, maximal PI responses to the various chimeric receptors were more strongly depressed than the corresponding cAMP responses, and carbachol showed considerably higher EC_{50} values in the PI assay. The apparent differences between the functional profiles of m2/m3-17aa and m3/m2-16aa can, thus, be interpreted without postulation of different structural determinants for both functional responses.

The results of the carbachol binding studies generally correlated well with the functional findings. In all cases, the GTP analog Gpp(NH)p produced a steepening and a rightward shift of the carbachol inhibition binding curves, consistent with all receptors being coupled to G proteins. Pretreatment of cells with PTX had no effect on carbachol binding to m3 and m2/m3-i3, whereas it quantitatively mimicked the effects of Gpp(NH)p in the case of m2 and m3/m2-i3. This finding is in agreement with the notion that the i3 loops determine the selectivity of G protein coupling. Interestingly, the carbachol IC_{50} values in the presence of Gpp(NH)p were similarly low for m2 and m3/m2-i3, whereas they were substantially higher for m3 and m2/m3-i3. This finding indicates that differences in carbachol binding affinities for the individual muscarinic receptors are mainly caused by the different i3 loops.

Consistent with the finding that m2/m3-17aa coupled to both PTX-sensitive and PTX-insensitive G proteins in the functional assays, the Gpp(NH)p effect on carbachol binding to this receptor was composed of a PTX-sensitive and a PTX-insensitive component. In the case of m3/m2-16aa, PTX had no significant effect on carbachol binding, although this receptor mediated a weak PTX-sensitive inhibition of cAMP levels in the functional assays. This discrepancy may be explained as follows. If only a small receptor fraction, which is sufficient to mediate a small cAMP response, is coupled to PTX-sensitive G proteins, these receptors may remain undetected in the carbachol binding assay. However, as already discussed in the previous paragraph, the binding studies in conjunction with the functional data suggest that m3/m2-16aa, similar to m2/m3-17aa, may be linked to both PTX-sensitive and PTX-insensitive G proteins.

It is conceivable that the large structural similarity found among all G protein-coupled receptors reflects a similar mode of interaction of the individual receptors with their respective G proteins. For this reason, the findings obtained in this study may be of general importance for the entire family of G protein-linked receptors.

References

1. Nathanson, N. M. Molecular properties of the muscarinic acetylcholine receptor. *Annu. Rev. Neurosci.* **10**:195–236 (1987).
2. Kubo, T., K. Fukuda, A. Mikami, A. Maeda, H. Takahashi, M. Mishina, T. Haga, K. Haga, A. Ichiyama, K. Kangawa, M. Kojima, H. Matsuo, T. Hirose, and S. Numa. Cloning, sequencing and expression of complementary DNA encoding the muscarinic acetylcholine receptor. *Nature (Lond.)* **323**:411–416 (1986).
3. Kubo, T., K. Maeda, K. Sugimoto, I. Akiba, A. Mikami, H. Takahashi, T. Haga, K. Haga, A. Ichiyama, K. Kangawa, H. Matsuo, T. Hirose, and S. Numa. Primary structure of porcine cardiac muscarinic acetylcholine receptor deduced from the cDNA sequence. *FEBS Lett.* **209**:367–372 (1986).
4. Peralta, E. G., J. W. Winslow, G. L. Peterson, D. H. Smith, A. Ashkenazi, J. Ramachandran, M. I. Schimerlik, and D. J. Capon. Primary structure and biochemical properties of an M_2 muscarinic receptor. *Science (Washington D. C.)* **236**:600–605 (1987).
5. Peralta, E. G., A. Ashkenazi, J. W. Winslow, D. H. Smith, J. Ramachandran, and D. J. Capon. Distinct primary structures, ligand-binding properties and tissue-specific expression of four human muscarinic acetylcholine receptors. *EMBO J.* **6**:3923–3929 (1987).
6. Bonner, T. I., N. J. Buckley, A. C. Young, and M. R. Brann. Identification of a family of muscarinic acetylcholine receptor genes. *Science (Washington D. C.)* **237**:527–532 (1987).
7. Bonner, T. I., A. C. Young, M. R. Brann, and N. J. Buckley. Cloning and expression of the human and rat m5 muscarinic acetylcholine receptor genes. *Neuron* **1**:403–410 (1988).
8. Shapiro, R. A., N. M. Scherer, B. A. Habecker, E. M. Subers, and N. M. Nathanson. Isolation, sequence, and functional expression of the mouse M1 muscarinic acetylcholine receptor gene. *J. Biol. Chem.* **263**:18397–18403 (1988).
9. Liao, C.-F., A. P. N. Themmen, R. Joho, C. Barberis, M. Birnbaumer, and L. Birnbaumer. Molecular cloning and expression of a fifth muscarinic acetylcholine receptor. *J. Biol. Chem.* **264**:7328–7337 (1989).
10. O'Dowd, B. F., R. J. Lefkowitz, and M. G. Caron. Structure of the adrenergic and related receptors. *Annu. Rev. Neurosci.* **12**:67–83 (1989).
11. Jones, S. V. P., J. L. Barker, N. J. Buckley, T. I. Bonner, R. M. Collins, and M. R. Brann. Cloned muscarinic receptor subtypes expressed in A9 L cells differ in their coupling to electrical responses. *Mol. Pharmacol.* **34**:421–426 (1988).
12. Fukuda, K., T. Kubo, I. Akiba, A. Maeda, M. Mishina, and S. Numa. Molecular distinction between muscarinic acetylcholine receptor subtypes. *Nature (Lond.)* **327**:623–625 (1987).
13. Conklin, B. R., M. R. Brann, N. J. Buckley, A. L. Ma, T. I. Bonner, and J. Axelrod. Stimulation of arachidonic acid release and inhibition of mitogenesis by cloned genes for muscarinic receptor subtypes stably expressed in A9 L cells. *Proc. Natl. Acad. Sci. USA* **85**:8698–8702 (1988).
14. Bujo, H., J. Nakai, T. Kubo, K. Fukuda, I. Akiba, A. Maeda, M. Mishina, and S. Numa. Different sensitivities to agonist of muscarinic acetylcholine receptor subtypes. *FEBS Lett.* **240**:95–100 (1988).
15. Neher, E., A. Marty, K. Fukuda, T. Kubo, and S. Numa. Intracellular calcium release mediated by two muscarinic receptor subtypes. *FEBS Lett.* **240**:88–94 (1988).
16. Fukuda, K., H. Higashida, T. Kubo, A. Maeda, I. Akiba, H. Bujo, M. Mishina, and S. Numa. Selective coupling with K^+ currents of muscarinic acetylcholine receptor subtypes in NG108-15 cells. *Nature (Lond.)* **335**:355–358 (1988).
17. Peralta, E. G., A. Ashkenazi, J. W. Winslow, J. Ramachandran, and D. J. Capon. Differential regulation of PI hydrolysis and adenylyl cyclase by muscarinic receptor subtypes. *Nature (Lond.)* **334**:434–437 (1988).
18. Jones, S. V. P., J. L. Barker, M. B. Goodman, and M. R. Brann. Inositol trisphosphate mediates cloned muscarinic receptor-activated conductances in transfected mouse fibroblast A9 L cells. *J. Physiol. (Lond.)* **421**:499–519 (1990).
19. Novotny, E. A., and M. R. Brann. Agonist pharmacology of cloned muscarinic receptors. *Trends Pharmacol. Sci.* **10**(suppl.):116 (1989).
20. Jones, S. V. P., T. J. Murphy, and M. R. Brann. Physiological comparison of cloned muscarinic receptor subtypes expressed in CHO cells. *Trends Pharmacol. Sci.* **10**(suppl.):116 (1989).
21. Ashkenazi, A., E. G. Peralta, J. W. Winslow, J. Ramachandran, and D. J. Capon. Functionally distinct G proteins selectively couple different receptors to PI hydrolysis in the same cell. *Cell* **56**:487–493 (1989).
22. Ashkenazi, A., J. W. Winslow, E. G. Peralta, G. L. Peterson, M. I. Schimerlik, D. J. Capon, and J. Ramachandran. An M2 muscarinic receptor subtype coupled to both adenylyl cyclase and phosphoinositide turnover. *Science (Washington D. C.)* **238**:672–675 (1987).
23. Kubo, T., H. Bujo, I. Akiba, J. Nakai, M. Mishina, and S. Numa. Location of a region of the muscarinic acetylcholine receptor involved in selective effector coupling. *FEBS Lett.* **241**:119–125 (1988).
24. Shapiro, R. A., B. T. Wakimoto, E. M. Subers, and N. M. Nathanson. Characterization and functional expression in mammalian cells of genomic and cDNA clones encoding a *Drosophila* muscarinic acetylcholine receptor. *Proc. Natl. Acad. Sci. USA* **86**:9039–9043 (1989).
25. Tietje, K. M., P. S. Goldman, and N. M. Nathanson. Cloning and functional analysis of a gene encoding a novel muscarinic acetylcholine receptor expressed in chick heart and brain. *J. Biol. Chem.* **265**:2828–2834 (1990).
26. Wess, J., M. R. Brann, and T. I. Bonner. Identification of a small intracellular region of the muscarinic m3 receptor as a determinant of selective coupling to PI turnover. *FEBS Lett.* **258**:133–136 (1989).
27. Okayama, H., and P. A. Berg. A cDNA cloning vector that permits expression of cDNA inserts in mammalian cells. *Mol. Cell. Biol.* **3**:280–289 (1983).
28. Chen, C., and H. Okayama. High-efficiency transformation of mammalian cells by plasmid DNA. *Mol. Cell. Biol.* **7**:2745–2752 (1987).
29. Buckley, N. J., T. I. Bonner, C. M. Buckley, and M. R. Brann. Antagonist binding properties of five cloned muscarinic receptors expressed in CHO-K1 cells. *Mol. Pharmacol.* **35**:469–476 (1989).
30. Bradford, M. M. A rapid and sensitive method for the quantitation of microgram quantities of protein utilizing the principle of protein dye binding. *Anal. Biochem.* **72**:248–254 (1976).
31. Berridge, M. J., M. C. Dawson, C. P. Downes, J. P. Heslop, and R. F. Irvine. Changes in the levels of inositol phosphates after agonist-dependent hydrolysis of membrane phosphoinositides. *Biochem. J.* **212**:473–482 (1983).
32. Felder, C. C., R. Y. Kanterman, A. L. Ma, and J. Axelrod. A transfected m1 muscarinic acetylcholine receptor stimulates adenylate cyclase via phosphatidylinositol hydrolysis. *J. Biol. Chem.* **264**:20356–20362 (1989).
33. Kobilka, B. K., T. S. Kobilka, K. Daniel, J. W. Regan, M. G. Caron, and R. J. Lefkowitz. Chimeric α_2-, β_2-adrenergic receptors: delineation of domains involved in effector coupling and ligand binding specificity. *Science (Washington D. C.)* **240**:1310–1316 (1988).
34. Shapiro, R. A., and N. M. Nathanson. Deletion analysis of the mouse m1 muscarinic acetylcholine receptor: effects on phosphoinositide metabolism and down-regulation. *Biochemistry* **28**:8946–8950 (1989).
35. Strader, C. D., R. A. F. Dixon, A. H. Cheung, M. R. Candelore, A. D. Blake, and I. S. Sigal. Mutations that uncouple the β-adrenergic receptor from G_s and increase agonist affinity. *J. Biol. Chem.* **262**:16439–16443 (1987).

Send reprint requests to: Jürgen Wess, Laboratory of Molecular Biology, NINDS-NIH, Bldg. 36, Rm. 3D-02, Bethesda, MD 20892.